Drive-Based Motivation for Coordination of Limit Cycle Behaviors

Craig Thompson Paul Reverdy

***Abstract*— Constructing autonomous systems capable of high-level behaviors often involves reducing these behaviors to a collection of low-level tasks. This requires developing a method for switching among possible tasks, for example using a hybrid automaton. Recent work has developed an alternative approach using continuous dynamical systems that have an internal drive state to select the desired task. In one particular result, authors considered a scenario where individual behaviors were encoded in control vector fields with unique, globally stable equilibria. A further level of complexity arises when one seeks to create a system that switches between tasks encoded as globally attracting sets with recurrent behaviors, rather than as point attractors. This work outlines the problem using the recently-developed drive-based dynamical framework. First we generalize the formulation of tasks as one part attracting set and one part recurrent behavior on said attracting set. Then as a proof-of-concept we demonstrate the existence of an attracting set consisting of orbits that repeatedly flow between two canonical limit cycles (e.g., Hopf oscillators).**

I. Introduction

A common approach to developing complex control systems is to construct a family of low-level controllers that encode individual behaviors and then construct a switching mechanism that allows the system to select an appropriate low-level controller, for example as a function of the system state. A commonly-used framework for developing the switching mechanism is that of the finite-state automaton. A system using a finite-state automaton to switch among a discrete set of continuous controllers is referred to as a hybrid automaton; such systems have been the subject of a large and growing body of literature [2]. In contrast, the problem of constructing a switching mechanism using a purely continuous dynamical system has received significantly less attention. This work is part of a larger project aimed at developing such a dynamical systems framework for switching among low-level controllers.

The switching system considered in this paper was first introduced by Reverdy and Koditschek [12]. In their paper they present a continuous dynamical system, which they term *motivation dynamics*, that switches between several different continuous low-level controllers. The motivation dynamics switching mechanism was inspired by previous work modeling decision making in animal groups [10], [13]. The modeling work has inspired an active body of controls research, e.g., [3], [14].

C. Thompson is with the Graduate Program in Applied Mathematics and P. Reverdy is with the Department of Aerospace and Mechanical Engineering, University of Arizona, Tucson, AZ 85721 USA. {craigthompson@math, preverdy@email}.arizona.edu.
This work has been supported in part by startup funds provided by the University of Arizona, as well as Air Force Research Laboratory grant FA8650-15-D-1845 subcontract 669737-6.

Both [12] and the present paper are inspired by applications in robotics, where navigation is a prototypical behavior. In robotics, *navigation* is understood to mean driving the system state to a desired value while avoiding forbidden regions which correspond to obstacles [5], [6]. In terms of dynamical systems, this corresponds to a flow with a single point attractor whose region of attraction consists of almost all the allowed points in the state space. Reverdy and Koditschek [12] study the motivation dynamics system with two low-level controllers that encode navigation tasks. They find sufficient conditions such that the overall system exhibits a limit cycle in which the system repeatedly visits the two point attractors in sequence. Such a recurrent behavior is of interest because it is a first step towards a family of more complex composite behaviors.

In this paper, we extend the results of [12] to a case where the low-level controllers encode a limit cycle. This extension is of interest for several reasons. First, while many possible tasks for an autonomous robot may be encoded as some form of point navigation, it might be more intuitive or convenient to encode tasks as a recurrent cycle, for instance: "follow this closed loop". Rather than form the desired path by navigating through a sequence of points around the circle, simply encode the entire behavior as a simpler mathematical object. Secondly, it is a proof of concept for extending the result of [12] to cases where there are many ($N > 2$) low-level navigation tasks and one desires a behavior where each of these tasks is performed repeatedly. Since the result of [12] provides a method to develop a limit cycle where the system repeatedly performs pairs ($N = 2$) of tasks, one way to develop such a behavior is to create a "limit cycle of limit cycles", i.e., a composite limit cycle consisting of several $N = 2$ limit cycles.

The extension we consider proceeds by generalizing the idea of a task to be one part navigation to an attracting set, and one part recurrent behavior on said set. First we lay the groundwork for this generalization, then we demonstrate it with a prototypical example: patrolling around a circle. Analytical results are derived in a symmetric case, and numerical results are shown for a more broad set of cases. The main technical contribution is the result presented as Theorem 4.4, which gives sufficient conditions for the generalized system to exhibit a supercritical Hopf bifurcation. In the post-bifurcation regime, the system has a limit cycle where the automaton oscillates between the two circles. Numerically we demonstrate that parameters can be relaxed such that the system repeatedly navigates around one circle, then the other.

The remainder of the paper is structured as follows. In Section II we present the system model for an arbitrary

number of low-level tasks, then specialize to the case of two tasks. In Section III we present the generalization of the low-level tasks to include a recurrent behavior, i.e., a limit cycle. In Section IV we reduce the dimensionality of the system using a singular perturbation argument and present the main result, Theorem 4.4, which shows the existence of a bifurcation in the resulting slow dynamics. In Section V we offer conclusions and suggestions for future work.

II. Model

A. General case.

The closed-loop system model is a coupled set of dynamical systems consisting of three main parts: spatial dynamics, motivation dynamics, and value dynamics.

The spatial dynamics determine the path of the robot. The motivation dynamics encode the robot's prioritization of its tasks. The value dynamics determine the current value of each task, which is then used to evolve the motivation of the robot. In an abstract sense, the spatial dynamics are plant dynamics for our control system. However, since our main application is robotics we model our system as a point particle with single-integrator dynamics in n-dimensional space. While we use this description for intuition, it is certainly possible to adapt these systems to a broader range of control problems.

We take x, m, and v to be the spatial, motivation, and value vectors, respectively. The vector x is our position in space, m_i is the motivation to pursue task i, and v_i is a positive metric associated with the value of task i. If we have k tasks being performed in $\mathbb{R}^n$ our system coordinates $\zeta = (x, m, v)$ live in $\mathbb{R}^n \times \Delta^k \times \mathbb{R}^k_+$, where Δ^k is the k-simplex, which we define as

$$\Delta^k := \left\{ (m, m_u) \in [0,1]^{k+1} \,\middle|\, m_u + \sum_{i=1}^{k} m_i = 1 \right\},$$

where m_u is the motivation to be "undecided", i.e., not to perform any task. While not intuitive, m_u is an important part of the motivation dynamics inherited from [13].

Our system is as follows: For x we have

$$\dot{x} = f_x(x, m) := \sum_{i=1}^{k} m_i \left(-\nabla \varphi_i(x) + R_i(x) \right). \tag{1}$$

For m we have

$$\begin{aligned} \dot{m}_i = f_{m,i}(m, v) &:= v_i^* v_i m_u \\ &\quad - m_i(1/(v_i^* v_i) - v_i^* v_i m_u + \sigma_i(1 - m_i - m_u)). \end{aligned} \tag{2}$$

For v we have

$$\dot{v}_i = f_{v,i}(v, x) := -\lambda_i (v_i - \varphi_i(x)). \tag{3}$$

Here, the function φ_i is called the *value function* for task i. In this scenario it is strictly increasing with the distance from x to the attracting set A_i associated with task i, and zero when $x \in A_i$. Thus φ_i is a Lyapunov function associated with our attracting set. The function R_i encodes a recurrent behavior on the set A_i. If we simply wish to navigate to A_i we will take $R_i \equiv 0$. The parameters v_i^*, σ_i, $\lambda_i > 0$ can all be adjusted to alter the characteristics of the task switching. Effectively, v_i^* is a gain on the value of task i, σ_i represents willingness to give up task i for another task, and λ_i is a timescale which controls how quickly v_i adjusts to reflect the value function φ_i.

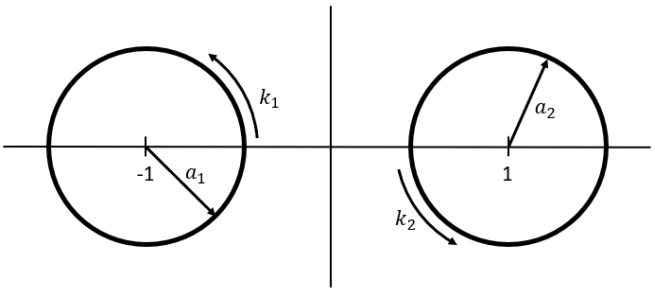

Fig. 1. Two circles, C_1, C_2, with radii a_1, a_2 and angular frequencies k_1, k_2.

The terms in (2) represent various forms of commitment and abandonment impulses. For a detailed description see [3] or [13]

The dynamics (1)–(3) mirror those of [12], except for the notable inclusion of the recurrent component R_i in the task vector fields.

We compactly represent our system as

$$\dot{\zeta} = f_\zeta(\zeta), \tag{4}$$

where $\zeta = (x, m, v)$ and $f_\zeta = (f_x, f_m, f_v)$.

B. Deadlock

Definition 2.1: A fixed point $\zeta = \zeta_d$ of (4) is a *deadlock* state if it is an asymptotically stable equilibrium. This deadlock is said to be *symmetric* if $m_1 = m_2 = \cdots = m_k =: m_d$ and $v_1 = v_2 = \cdots = v_k =: v_d$.

C. Two task case.

We limit our discussion to the case of two tasks in $\mathbb{R}^2$. This is by no means restrictive, as there is a rich set of behaviors that can be demonstrated with just two tasks. Moreover, we consider the case of symmetric motivation and value. That is, we take our parameters to be independent of task, i.e. $v_1^* = v_2^* = 1/\varepsilon_v$, $\lambda_1 = \lambda_2 = 1/\varepsilon_\lambda$, and $\sigma_1 = \sigma_2 = \sigma$. Here we have chosen the ε notation as we intend to perform a singular perturbation analysis on these parameters later in this paper.

III. Two circular limit cycles

Now we consider the case of our tasks no longer being "navigate to point $x^{(i)}$" but instead "patrol on circle C_i with angular velocity k_i" (e.g. Fig. 1). This requires a generalization as our desired behavior cannot be phrased as the result of a gradient system. This is why we have added the recurrence function R_i to the system from [12].

We want $\varphi_i(x)$ to increase with the minimum distance to the attracting set. For a circle centered at point $x_*^{(i)}$ with radius a_i we take

$$\varphi_i(x) = \frac{1}{4}\left(a_i^2 - \|x - x_*^{(i)}\|^2 \right)^2 \quad i = 1, 2.$$

Proper choice of $R_i(x)$ will induce rotational dynamics on C_i. Here we take

$$R_i(x) = \begin{pmatrix} -k_i(x_2 - x_{*2}^{(i)}) \\ k_i(x_1 - x_{*1}^{(i)}) \end{pmatrix} \quad i = 1, 2,$$

which will cause a constant rotation with angular frequency k_i. Note that $\nabla\varphi_i(x) \cdot R_i(x) = 0$. Thus the addition of R_i does not affect the location of the attracting set. With this construction the expression

$$-\nabla\varphi_i(x) + R_i(x)$$

defines a circular Hopf oscillator centered at $x^{(i)}$. Thus we may think of $f_x(x, m)$ as the linear combination of Hopf oscillator vector fields.

We will consider $x_*^{(1)} = (-1, 0)$ and $x_*^{(2)} = (1, 0)$. This is an acceptable simplification as the stability properties of the system are robust to translations and rotations, which results in no effective loss of generality. However, we will only consider when the circles C_1 and C_2 do not intersect, as the intersecting case is far more complex.

A. Conversion To Sum/Difference Coordinates

It is valuable to view the system in terms of sum and difference coordinates and parameters. This transformation gives more insight to the symmetries of the system. Thus we will take $m_+ = m_1 + m_2$, $m_- = m_1 - m_2$, and define v_+, v_-, a_+, a_-, k_+, and k_- in a similar fashion. Note that this is analogous to the notation in [12], except $m_+ = 2\bar{m}$. Additionally, we will consider the symmetric case when $a_- = k_- = 0$. Making this change of coordinates creates the following transformed system:

$$\begin{aligned} \dot{x}_1 = \frac{1}{4}\big[m_+(x_1(a_+^2 - 4(3 + x_1^2 + x_2^2)) \\ - 2k_+x_2) \\ +m_-(a_+^2 - 4(1 + 3x_1^2 + x_2^2))\big] \end{aligned} \tag{5}$$

$$\begin{aligned} \dot{x}_2 = \frac{1}{4}\big[m_+(x_2(a_+^2 - 4(1 + x_1^2 + x_2^2)) \\ + 2k_+x_1) \\ +m_-(2k_+ - 8x_1x_2)\big] \end{aligned} \tag{6}$$

$$\begin{aligned} \dot{m}_- = \frac{1 - m_+}{2\varepsilon_v}(m_-v_+ + v_-(2 + m_+)) \\ - 2\varepsilon_v\frac{m_+v_- - m_-v_+}{v_-^2 - v_+^2} \end{aligned} \tag{7}$$

$$\begin{aligned} \dot{m}_+ = \frac{1 - m_+}{2\varepsilon_v}(m_-v_- + v_+(2 + m_+)) \\ + \frac{1}{2}\sigma(m_-^2 - m_+^2) \\ - 2\varepsilon_v\frac{m_-v_- - m_+v_+}{v_-^2 - v_+^2} \end{aligned} \tag{8}$$

$$\dot{v}_- = \frac{1}{\varepsilon_\lambda}(\varphi_-(x) - v_-) \tag{9}$$

$$\dot{v}_+ = \frac{1}{\varepsilon_\lambda}(\varphi_+(x) - v_+) \tag{10}$$

Here $\varphi_+ = \varphi_1 + \varphi_2$ and $\varphi_- = \varphi_1 - \varphi_2$. Compactly we have the system

$$\dot{z} = f(z), \tag{11}$$

where $z = (x_1, x_2, m_-, m_+, v_-, v_+)$ and $f_z = (f_{x_1}, f_{x_2}, f_{m_-}, f_{m_+}, f_{v_-}, f_{v_+})$.

In the two-task case, under the sum/difference coordinates transformation, we have symmetric deadlock at an asymptotically stable fixed point z_d of (11) when $z_d = (x_{d,1}, x_{d,2}, 0, 2m_d, 0, 2v_d)$.

From here we analyze properties of our system. In particular, we show that, in the limit as $\varepsilon_v, \varepsilon_\lambda \to 0$ there are values of $\sigma > 0$ such that we avoid deadlock.

IV. Reduction of the system in the singular perturbation limit.

In this section we study the limit $\varepsilon_v, \varepsilon_\lambda \to 0$ using singular perturbation techniques and demonstrate that the system can break deadlock when the parameter σ crosses a critical value σ^*. As a preliminary step, we show the existence of a bounded positive invariant attracting set for the dynamics.

A. Attracting set.

Theorem 4.1: Let $\mathcal{M} = \mathbb{R}^2 \times \Delta^2 \times \mathbb{R} \times \mathbb{R}_+$ and fix $a_+ \in [0, 2)$. Let A be given by

$$A := 1 + \sqrt{\frac{a_+^2 + \sqrt{a_+^4 + 4k_+^2}}{8}}. \tag{12}$$

Then there exists $\delta, \varepsilon > 0$ such that

$$\begin{aligned} \mathcal{A} := \{z \in \mathcal{M} | v_+ \geq \delta, m_+ > \varepsilon, \\ x \in [-A, A] \times [-A + 1, A - 1]\} \end{aligned} \tag{13}$$

is a positive invariant attracting set under the dynamics (11).

Proof: First note that $\varphi_i(x) > 0$ for x not on circle C_i. Thus if we have non-intersecting circles, i.e. $a_+ \in [0, 2)$, then $\varphi_+(x) = \varphi_1(x) + \varphi_2(x) > 0$ for all x. Moreover, for a fixed a_+ there exists an $\delta > 0$ such that $\varphi_+(x) > \delta$. Thus we have that

$$\dot{v}_+|_{v_+ = \delta} = 1/\varepsilon_\lambda(\varphi_+(x) - \delta) > 0.$$

Thus the set $\{z \in \mathcal{M} | v_+ \geq \delta\}$ is attracting positive invariant. Furthermore we have that $m_+ \geq 0$ by definition, and that $|m_-| \leq m_+$. Thus $m_+ = 0$ implies $m_- = 0$ and

$$\dot{m}_+|_{m_+ = 0} = \frac{v_+}{\varepsilon_v} > 0$$

for $v_+ \geq \delta$. Thus by the continuity of (8) there exists $\varepsilon > 0$ such that $\dot{m}_+ > 0$ for $m_+ < \varepsilon$. This makes $\{z \in \mathcal{M} | m_+ > \varepsilon\}$ an attracting positive invariant set.

Now we show that there is an attracting positive invariant set for the spatial coordinates $x = (x_1, x_2)$, dependent on a_+ and k_+. For the sake of brevity, we will only prove the upper bound for x_1 here. The lower bound is an entirely analogous proof. The proof of bounds for x_2 involves some extra considerations but follows a very similar procedure. A proof of the bounds for x_2 can be found in Appendix I.

Let $x_1 > a_+/2 + 1$, then $a_+^2 - 4x_1^2 < 0$. Using this and the fact that $|m_-| \leq m_+$ we may write

$$\begin{aligned}
4\dot{x}_1 &= m_+(x_1(a_+^2 - 4(3 + x_1^2 + x_2^2)) - 2k_+x_2) \\
&\quad + m_-(a_+^2 - 4(1 + 3x_1^2 + x_2^2)) \\
&\leq m_+[x_1(a_+^2 - 4(3 + x_1^2 + x_2^2)) - 2k_+x_2) \\
&\quad - (a_+^2 - 4(1 + 3x_1^2 + x_2^2))] \\
&= m_+[-4(x_1 - 1)x_2^2 - 2k_+x_2 \\
&\quad - 4(x_1 - 1)^3 + (x_1 - 1)a_+^2].
\end{aligned}$$

What we obtain is a quadratic polynomial in x_2. The corresponding parabola opens down, and so we are bounded above by its vertex:

$$\begin{aligned}
&-4(x_1 - 1)x_2^2 - 2k_+x_2 - 4(x_1 - 1)^3 + (x_1 - 1)a_+^2 \\
&\leq -4(x_1 - 1)^3 + (x_1 - 1)a_+^2 + \frac{k_+^2}{4(x_1 - 1)}.
\end{aligned}$$

If we solve for the expression on the right-hand-side to be negative we obtain the bound $x_1 > A$, where A is given by (12) This bound ensures that $\dot{x}_1 < 0$. Also note that $x_1 > A$ satisfies the assumption that $x_1 > a_+/2 + 1$.

The lower bound of the system is symmetric and we have that $x_1 < -A$ implies that $\dot{x}_1 > 0$. Thus the set $\{z \in \mathcal{M} | x_1 \in [-A, A]\}$ is attracting positive-invariant. Along with the bounds for $\dot{x}_2$ derived in Appendix I we obtain the attracting positive invariant set $\{z \in \mathcal{M} | x_2 \in [-A + 1, A - 1]\}$. The intersection of all of these sets gives our set $\mathcal{A}$ as given in (13). ∎

B. Three-dimensional slow dynamics in the singular limit.

We wish to study the limit $\varepsilon_v, \varepsilon_\lambda \to 0$ in the form of a singular perturbation problem. Intuitively this is equivalent to taking the value gain v^* to infinity (pursuing a task is infinitely more valuable than being undecided), and taking the time scale constant λ to infinity (the value variable v_i directly reflects its respective value function φ_i). Following the technique of [12] we couple our parameters by taking $\varepsilon_\lambda = c\varepsilon_v$ where $c > 0$. We split our variables into slow, $w = (x_1, x_2, m_-)$, and fast, $y = ((1 - m_+)/\varepsilon_v, v_-, v_+)$. The dynamics of the slow variable w are given by

$$\begin{aligned}
\dot{w}_1 &= \frac{1}{4}\left[(1 - \varepsilon_v y_1)(w_1(a_+^2 - 4(3 + w_1^2 + w_2^2)) \right. \\
&\qquad - 2k_+w_2) \\
&\qquad \left. + w_3(a_+^2 - 4(1 + 3w_1^2 + w_2^2))\right],
\end{aligned} \tag{14}$$

$$\begin{aligned}
\dot{w}_2 &= \frac{1}{4}\left[(1 - \varepsilon_v y_1)(w_2(a_+^2 - 4(1 + w_1^2 + w_2^2)) \right. \\
&\qquad + 2k_+w_1) \\
&\qquad \left. + w_3(2k_+ - 8w_1w_2)\right],
\end{aligned} \tag{15}$$

$$\begin{aligned}
\dot{w}_3 &= \frac{y_1}{2}(w_3y_3 + y_2(3 - \varepsilon_v y_1)) \\
&\quad - 2\varepsilon_v \frac{(1 - \varepsilon_v y_1)y_2 - w_3y_3}{y_2^2 - y_3^2},
\end{aligned} \tag{16}$$

and those of the fast variable y are given by

$$\begin{aligned}
\varepsilon_v\dot{y}_1 &= -\frac{y_1}{2}(w_3y_2 + y_3(3 - \varepsilon_v y_1)) \\
&\quad - \frac{1}{2}\sigma(w_3^2 - (1 - \varepsilon_v y_1)^2) \\
&\quad + 2\varepsilon_v \frac{w_3y_2 - (1 - \varepsilon_v y_1)y_3}{y_2^2 - y_3^2},
\end{aligned} \tag{17}$$

$$\varepsilon_v\dot{y}_2 = \frac{1}{c}(\varphi_-(w) - y_2), \tag{18}$$

$$\varepsilon_v\dot{y}_3 = \frac{1}{c}(\varphi_+(w) - y_3). \tag{19}$$

Lemma 4.2: In the singular limit $\varepsilon_v \to 0$ the system given by (14)–(19) reduces to the three dimensional system (23).

Proof: Take $\varepsilon_v \to 0$ to obtain solutions of (17)–(19):

$$y_1 = \sigma\frac{(1 - w_3^2)}{3\varphi_+(w) + w_3\varphi_-(w)}, \tag{20}$$

$$y_2 = \varphi_-(w) \tag{21}$$

$$y_3 = \varphi_+(w) \tag{22}$$

Substituting these back into the slow dynamics along with the ε_v limit yields

$$\begin{aligned}
\dot{w}_1 &= \frac{1}{4}\left[(w_1(a_+^2 - 4(3 + w_1^2 + w_2^2)) \right. \\
&\qquad - 2k_+w_2) \\
&\qquad \left. + w_3(a_+^2 - 4(1 + 3w_1^2 + w_2^2))\right], \\
\dot{w}_2 &= \frac{1}{4}\left[(w_2(a_+^2 - 4(1 + w_1^2 + w_2^2)) \right. \\
&\qquad + 2k_+w_1) \\
&\qquad \left. + w_3(2k_+ - 8w_1w_2)\right], \\
\dot{w}_3 &= \frac{\sigma(1 - w_3^2)(w_3\varphi_+(w) + 3\varphi_-(w))}{6\varphi_+(w) + 2w_3\varphi_-(w)},
\end{aligned} \tag{23}$$

∎

For $a_+ \in [0, 2)$ the fixed points of our system are $w = (1, 0, -1), (-1, 0, 1), (0, 0, 0)$. One can show that these must be the only fixed points, but since that proof is not key to the main result and space is limited we will omit it.

Lemma 4.3: The fixed points $w = (1, 0, -1)$, and $w = (-1, 0, 1)$ are unstable for all $a_+ \geq 0$, $\sigma > 0$ and k_+.

Proof: Let $w = (1, 0, -1)$ or $(-1, 0, 1)$. In either case, the Jacobian of the system is

$$\begin{pmatrix}
\frac{a_+^2}{4} & \frac{k_+}{2} & 0 \\
-\frac{k_+}{2} & \frac{a_+^2}{4} & 0 \\
\frac{a_+^2}{4} - 4 & \frac{k_+}{2} & \frac{\left(512 - (a_+^2 + 16)^2\right)\sigma}{512 + (3a_+^2 + 16)(a_+^2 - 16)}
\end{pmatrix}$$

The eigenvalues are

$$\mu_1 = \frac{1}{4}(a_+^2 + 2ik_+), \quad \mu_2 = \frac{1}{4}(a_+^2 - 2ik_+),$$

$$\text{and} \quad \mu_3 = \frac{\left(512 - (a_+^2 + 16)^2\right)\sigma}{512 + (3a_+^2 + 16)(a_+^2 - 16)}$$

The first two have strictly positive real part when $a_+ > 0$, and when $a_+ = 0$ we have that $\mu_3 > 0$. Thus we are unstable for all $a_+ \geq 0$ and k_+. This means that we cannot experience deadlock at either of these fixed points. ■

The third fixed point, $w = (0, 0, 0)$ is where we have a potential for deadlock. Specifically, the system undergoes a supercritical Hopf bifurcation as σ is raised through a critical value. We formalize this in the following theorem. Since the two circle limit cycles example is primarily a proof of concept we will now further simplify to the case of $a_+ = 1$ and $k_+ = 2$, for the sake of algebraic simplicity (each radius is $\frac{1}{2}$ with an angular frequency of 1). However, we have numerically verified that a critical σ-value exists for a wide range of a_+ and k_+ values. Additionally.

Theorem 4.4: In the slow dynamics (23) with $a_+ = 1$ and $k_+ = 2$, a supercritical Hopf bifurcation occurs at the fixed point $w = (0, 0, 0)$ as σ is raised through the bifurcation value σ^*, where σ^* is given by

$$\sigma^* = \frac{3}{34}\left(12\sqrt{43} + 19\right) \approx 8.6. \tag{24}$$

Proof: We demonstrate that we satisfy the conditions in the Hopf bifurcation theorem described in Appendix II. The Jacobian of (23) is

$$J(\sigma) = \begin{pmatrix} -\frac{11}{4} & 1 & \frac{8\sigma}{3} \\ -1 & -\frac{3}{4} & 0 \\ -\frac{3}{4} & 1 & \frac{\sigma}{6} \end{pmatrix}$$

The eigenvalues at σ^* are $\nu_1 = \frac{3}{68}\left(4\sqrt{43} - 73\right) < 0$, $\nu_2 = -\frac{1}{4}i\sqrt{24\sqrt{43} + 87}$, and $\nu_3 = \frac{1}{4}i\sqrt{24\sqrt{43} + 87}$. Thus we satisfy the first condition, as we have a pair of pure imaginary eigenvalues and all other eigenvalues have nonzero real-part. In addition, $d(\text{Re } \nu_2(\sigma))/d\sigma|_{\sigma=\sigma^*} \neq 0$. The first Lyapunov coefficient, ℓ_1, can be computed in closed form and is negative. We do not present the computation here due to space constraints. Thus, along with the first condition, we have a supercritical Hopf bifurcation. ■

Finally, we can also show that for *any* choice of non-intersecting attracting sets, there exists a value of σ where there is no deadlock point in the system.

C. Numerical results

Theorem 4.4 shows that the slow dynamics (23) undergo a supercritical Hopf bifurcation for a particular value of the parameters a_+ and k_+. Numerical study suggests that the supercritical Hopf bifurcation exists for all values of $a_+ \in [0, 2)$ and many values of $k_+ > 0$ (see Fig. 2). Moreover, it appears that there is a limiting curve $\sigma^* = \sigma(a_+)$ for the limit $k_+ \to \infty$. Thus, we have strong reason to believe that the result of Theorem 4.4 holds in a large region of the parameter space.

In addition to avoiding deadlock in the singular perturbation limit, numerical study also shows that when ε_λ is relaxed we can produce a limit cycle with more "desirable" behavior. That is, we produce a cycle in which the automaton patrols the perimeter of each circle once (approximately) before switching to the other circle (See Fig. 3).

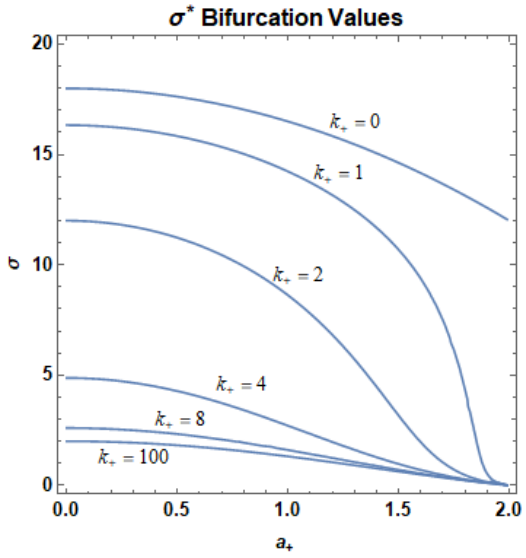

Fig. 2. In each case, the supercritical Hopf bifurcation occurs when raising σ past the critical value given by the curve. Curves are plotted for $k_+ = 0, 1, 2, 4, 8, 100$.

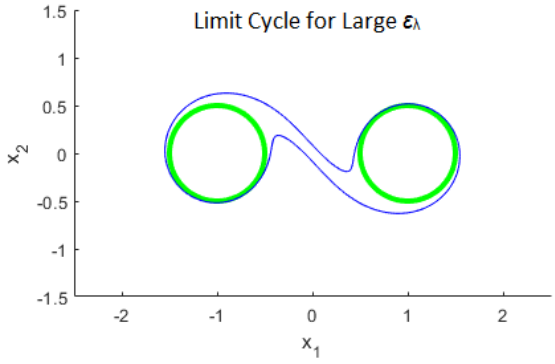

Fig. 3. Numerically determined limit cycle for parameter values $\sigma = 9$, $\varepsilon_v = 0.001$, and $\varepsilon_\lambda = 6$. The thin blue line is the limit cycle path of the automaton. The thick green circles indicate C_1 (left) and C_2 (right).

V. Conclusion and Future Work.

We have shown that, with proper choice of parameters, our system can avoid deadlock in the case of two disjoint limit cycles. The resulting system dynamics consists of a limit cycle where the spatial state x repeatedly oscillates between the two low-level circular limit cycles. Future work in this direction includes

1) proving results for fully general limit cycles,
2) studying parameter regimes where ε_v and ε_λ are not limiting to 0,
3) and extending to an arbitrary number of tasks.

The work presented in this paper advances the goal of developing a dynamical systems framework for switching among low-level controllers to achieve a high-level behavior. In applications, it is desirable to be able to specify this behavior in an appropriately abstract but expressive programming language. When the switching mechanism is a finite-state automaton, temporal logics such as linear temporal logic

(LTL) [1], [7], [8] and more recently, signal temporal logic (STL) [11] have proven to be effective at expressing high-level behaviors. Specifically, these logics admit computational tools which synthesize hybrid automata that realize these behaviors. Our eventual goal is to be able to provide an equivalent interface and synthesis tools for switching mechanisms based on motivation dynamics.

One such method of synthesis is to optimize over the set of possible parameter values. The parameters used in the general model (4) (i.e. v_i^*, λ_i, and σ_i) can be tuned to produce a variety of interesting behaviors. These behaviors have some quantifiable properties, such as the number of patrols around each circle, but determining proper parameter regimes is very system dependent. One solution is to use STL methods to measure the "success" (see Maler and Nickovic [9]) of parameter combinations, and then optimize over the space of parameter values. From there, one can consider synthesizing the "best" automaton for accomplishing a set of tasks encoded as STL formulas.

APPENDIX I
BOUNDS FOR $\dot{x}_2$

Lemma: Let $\mathcal{M} \coloneqq \mathbb{R}^2 \times \Delta^2 \times \mathbb{R} \times \mathbb{R}_+$ and define A by (12). Then, if $\dot{x}_2$ is given by (6), $x_2 > A-1 \implies \dot{x}_2 < 0$ and $x_2 < -A+1 \implies \dot{x}_2 > 0$. Thus the set

$$\{z \in \mathcal{M} | x_2 \in [-A+1, A-1]\}$$

is a positive invariant attracting subset of $\mathcal{M}$ under the dynamics given by (11).

Proof: We will prove the case for the upper bound of x_2. The lower case is analogous. First note that if $x_2 > A-1$ then $a_+^2 - 4x_2^2 < 0$. Then note that there are two cases to consider, depending on whether the last term in (6), $(2k_+ - 8x_1x_2)$, is negative or positive. Thus we have the following case dependent bound:

$$\begin{aligned}
4\dot{x}_2 &= m_+(x_2(a_+^2 - 4(1+x_1^2+x_2^2)) + 2k_+x_1) \\
&\quad + m_-(2k_+ - 8x_1x_2) \\
&\leq m_+(x_2(a_+^2 - 4(1+x_1^2+x_2^2)) + 2k_+x_1) \\
&\quad + \begin{cases} m_+(2k_+ - 8x_1x_2) & \text{if } x_1 \leq \frac{k_+}{4x_2} \\ -m_+(2k_+ - 8x_1x_2) & \text{if } x_1 > \frac{k_+}{4x_2} \end{cases} \\
&= m_+[x_2(a_+^2 - 4((x_1 \pm 1)^2 + x_2^2)) + 2k_+(x_1 \pm 1)] \\
&= m_+[-4x_2(x_1 \pm 1)^2 + 2k_+(x_1 \pm 1) - 4x_2^3 + a_+^2 x_2]
\end{aligned}$$

Here the plus case is $x_1 \leq \frac{k_+}{4x_2}$ and the minus case is $x_1 > \frac{k_+}{4x_2}$. Just as in the proof for the x_1 bounds, we have an expression which is quadratic, this time in the variable $(x_1 \pm 1)$. From here the method of solution is the same as that in section IV-A. ∎

APPENDIX II
HOPF BIFURCATION THEOREM.

Theorem: (Theorem 3.4.2 from [4]) Suppose that the system $\dot{z} = f(z, \mu)$; $z \in \mathbb{R}^n$, $\mu \in \mathbb{R}$, has an equilibrium $(z_0; \mu_0)$ and the following properties are satisfied:

1) The Jacobian $D_z f|_{(z_0,\mu_0)}$ has a simple pair of pure imaginary eigenvalues $\lambda(\mu_0)$ and $\bar{\lambda}(\mu_0)$ and no other eigenvalues with zero real parts,
2) $d(Re\lambda(\mu))/d\mu|_{\mu=\mu_0} = d \neq 0$

Property 1) implies that there is a smooth curve of equilibria $(z(\mu), \mu)$ with $z(\mu_0) = z_0$. The eigenvalues $\lambda(\mu_0)$, $\bar{\lambda}(\mu_0)$ of $D_z f|_{(z_0,\mu_0)}$ which are imaginary at $\mu = \mu_0$ vary smoothly with μ.

If Property 2) is satisfied, then there is a unique three-dimensional center manifold passing through (z_0, μ_0) in $\mathbb{R}^n \times \mathbb{R}$ and a smooth system of coordinates (preserving the planes $\mu = const.$) for which the Taylor expansion of degree 3 on the center manifold is given by [4, (3.4.8)]. If$\ell_1|_{(z_0,\mu_0)} = 0$, there is a surface of periodic solutions in the center manifold which has quadratic tangency with the eigenspace of $\lambda(\mu_0)$, $\bar{\lambda}(\mu_0)$ agreeing to second order with the paraboloid $\mu = -(\ell_1|_{(z_0,\mu_0)}/d)(x^2+y^2)$. If $\ell_1|_{(z_0,\mu_0)} < 0$, then these periodic solutions are stable limit cycles, while if $\ell_1|_{(z_0,\mu_0)} > 0$, the periodic solutions are repelling.

REFERENCES

[1] G. E. Fainekos, A. Girard, H. Kress-Gazit, and G. J. Pappas. Temporal logic motion planning for dynamic robots. *Automatica*, 45(2):343–352, 2009.

[2] R. Goebel, R. G. Sanfelice, and A. R. Teel. *Hybrid Dynamical Systems: modeling, stability, and robustness*. Princeton University Press, 2012.

[3] R. Gray, A. Franci, V. Srivastava, and N. E. Leonard. Multi-agent decision-making dynamics inspired by honeybees. *IEEE Transactions on Control of Network Systems*, 5(2):793–806, 2018.

[4] J. Guckenheimer and P. J. Holmes. *Nonlinear oscillations, dynamical systems, and bifurcations of vector fields*, volume 42 of *Applied Mathematical Sciences*. Springer Science & Business Media, 2013.

[5] O. Khatib. Real-time obstacle avoidance for manipulators and mobile robots. *The International Journal of Robotics Research*, 5(1):90–98, Mar 1986.

[6] D. E. Koditschek and E. Rimon. Robot navigation functions on manifolds with boundary. *Advances in applied mathematics*, 11(4):412–442, 1990.

[7] H. Kress-Gazit, G. E. Fainekos, and G. J. Pappas. Temporal-logic-based reactive mission and motion planning. *IEEE Transactions on Robotics*, 25(6):1370–1381, 2009.

[8] J. Liu, N. Ozay, U. Topcu, and R. M. Murray. Synthesis of reactive switching protocols from temporal logic specifications. *IEEE Transactions on Automatic Control*, 58(7):1771–1785, 2013.

[9] O. Maler and D. Nickovic. Monitoring temporal properties of continuous signals. In *Formal Techniques, Modelling and Analysis of Timed and Fault-Tolerant Systems*, pages 152–166. Springer, 2004.

[10] D. Pais, P. M. Hogan, T. Schlegel, N. R. Franks, N. E. Leonard, and J. A. Marshall. A mechanism for value-sensitive decision-making. *PloS one*, 8(9):e73216, 2013.

[11] V. Raman, A. Donzé, D. Sadigh, R. M. Murray, and S. A. Seshia. Reactive synthesis from signal temporal logic specifications. In *Proceedings of the 18th International Conference on Hybrid Systems Computation and Control - HSCC '15*, pages 239–248, Seattle, Washington, 2015. ACM Press.

[12] P. Reverdy and D. E. Koditschek. A dynamical system for prioritizing and coordinating motivations. *SIAM Journal on Applied Dynamical Systems*, 17(2):1683–1715, 2018.

[13] T. D. Seeley, P. K. Visscher, T. Schlegel, P. M. Hogan, N. R. Franks, and J. A. Marshall. Stop signals provide cross inhibition in collective decision-making by honeybee swarms. *Science*, 335(6064):108–111, 2012.

[14] L. Stella and D. Bauso. Bio-inspired evolutionary dynamics on complex networks under uncertain cross-inhibitory signals. *Automatica*, 100:61 – 66, 2019.